Published in final edited form as:
Environ Mol Mutagen. 2011 January ; 52(1): 58–68. doi:10.1002/em.20581.

Assessment of Multiple Types of DNA Damage in Human Placentas from Smoking and Non-smoking Women in the Czech Republic

M. Margaret Pratt[1,+,*], **Leon C. King**[2,+], **Linda D. Adams**[2], **Kaarthik John**[1], **Paul Sirajuddin**[1], **Ofelia A. Olivero**[1], **David K. Manchester**[3], **Radim J. Sram**[4], **David M. DeMarini**[2], and **Miriam C. Poirier**[1]

[1]Carcinogen-DNA Interactions Section, LCBG, Center for Cancer Research, National Cancer Institute, NIH, Bethesda, MD, U.S.A.

[2]Integrated Systems Toxicology Division, U.S. Environmental Protection Agency, Research Triangle Park, NC, U.S.A.

[3]University of Colorado Denver School of Medicine, Clinical Genetics and Metabolism, The Children's Hospital, Aurora, CO, U.S.A.

[4]Institute of Experimental Medicine, Academy of Sciences of the Czech Republic, Prague, Czech Republic

Abstract

Three classes of DNA damage were assessed in human placentas collected (in 2000-4) from 51 women living in the Teplice region of the Czech Republic, a mining area considered to have some of the worst environmental pollution in Europe in the 1980s. Polycyclic aromatic hydrocarbon (PAH)-DNA adducts were localized and semiquantified using immunohistochemistry (IHC) and the Automated Cellular Imaging System (ACIS). More generalized DNA damage was measured both by ^{32}P-postlabeling and by abasic (AB) site analysis. Placenta stained with antiserum elicited against DNA modified with r7, t8-dihydroxy-t-9, 10-oxy-7,8,9,10-tetrahydro-benzo[*a*]pyrene (BPDE) revealed PAH-DNA adduct localization in nuclei of the cytotrophoblast (CT) cells and syncytiotrophoblast (ST) knots lining the chorionic villi. The highest levels of DNA damage, 49–312 PAH-DNA adducts/10^8 nucleotides, were found by IHC/ACIS in 14 immediately-fixed placenta samples. An additional 37 placenta samples were stored frozen before fixation and embedding, and because PAH-DNA adducts were largely undetectable in these samples, freezing was implicated in the loss of IHC signal. The same placentas (n = 37) contained 1.7 – 8.6 stable/bulky DNA adducts/10^8 nucleotides and 0.6 – 47.2 AB sites/10^5 nucleotides. For all methods there was no correlation among types of DNA damage and no difference in extent of DNA damage between smokers and non-smokers. Therefore, the data show that DNA from placentas obtained in Teplice contained multiple types of DNA damage, which likely arose from various environmental exposures. In addition, PAH-DNA adducts were present at high concentrations in the CT cells and ST knots of the chorionic villi.

Keywords

Automated Cellular Imaging System; Immunohistochemistry; BPDE-DNA antiserum; Abasic sites; ^{32}P-Postlabeling; Teplice Program

[*]Corresponding author at: National Cancer Institute, 37 Convent Drive, Building 37, Room 4032, National Institutes of Health, Bethesda, MD, U.S.A.. Tel.: +1 301 435 4527; fax: +1 301 402 0153, m2pratt@yahoo.com.
[+]Co-first authors who contributed equally to this study.

Introduction

Airborne pollution has been implicated in a host of pulmonary and other detrimental health effects in humans [Lewtas, 2007]. Polycyclic aromatic hydrocarbons (PAHs), produced by incomplete combustion, are major constituents of airborne pollution and concentrate near combustion sources, such as automobiles, homes burning coal or wood, and industrial sites [Lewtas, 2007]. In the 1980s, the mining regions of Northern Bohemia, in what is now the Czech Republic, were considered to be among the most polluted in all of Europe [Binkova et al., 2003; Sram, 2001]. In the early 1990s a series of studies known as the Teplice Program was undertaken in Northern Bohemia, in the area surrounding the city of Teplice, to evaluate the levels of pollutants and their associations with previously noted adverse health outcomes. These included mortality, incidences of respiratory disease, immune-deficiencies, cardiovascular disease, and cancer in adults [Sram, 2001]. In addition, there were neurobehavioral disorders in children and adverse effects on pregnancy outcome because children born in this region were at increased risk for intrauterine growth retardation (IUGR), low birth weight, and morphologically abnormal placentas [Sram, 2001]. The results of this study support a growing body of evidence that airborne pollutants, including particulate matter, may damage DNA and induce adverse effects in both mother and fetus [Dejmek et al., 1999; Dejmek, 2000; Sram et al., 1999].

Because PAH-DNA adduct formation is an indicator of PAH exposure [Rothman et al., 1990; Rothman et al., 1993b; Rothman et al., 1993a] and is associated with IUGR [Dejmek et al., 1999; Dejmek, 2000], we examined placentas taken from women in Teplice for evidence of PAH-DNA adduct formation. The placental chorionic villi are finger-like projections that extend into the maternal blood supply, allowing passage of nutrients and filtering out impurities to protect the infant [Cross et al., 2006]. The chorionic villi are lined on the outside surface with syncytiotrophoblasts (ST), which include knots of bound nuclei, and, below the syncytium, mononucleated cytotrophoblast (CT) cells. Both ST and CT cells contain xenobiotic metabolizing enzymes that are involved in the bioactivation of PAHs. The effectiveness of metabolism in this tissue and the range of xenobiotics metabolized are not well understood. However, for this study we hypothesized that ST and CT cells would have the highest concentration of PAH-DNA adducts in the human placenta.

Because the placenta likely metabolizes all incoming xenobiotic insults, we also hypothesized that placental tissue would have evidence of exposure to different types of DNA damaging agents. Therefore, this study examined 3 distinct endpoints, two of which result from damage that is not limited to PAH-DNA adduct formation. An antibody with specificity for PAH-DNA was used to stain placenta tissue for localization of adducts by immunohistochemistry (IHC) with semiquantitation using the Automated Cellular Imaging System (ACIS). Stable/bulky DNA adducts that include, but are not limited to those formed by reaction with PAHs, were detected and quantified by ^{32}P-postlabeling. Abasic (AB) sites, which can occur spontaneously and from ionizing radiation, also result from attempts to repair alkylated DNA.

Materials and methods

Human subjects and tissue procurement

Human placentas were collected, following full-term pregnancy and normal delivery, from two separate groups of women designated Group 1 (n = 14) and, Group 2 (n = 37). All samples were from women living in the Teplice region of the Czech Republic. Smoking status and exposure to environmental tobacco smoke (ETS) were self-reported for both groups. Informed consent was obtained under the prevailing institutional review board

guidelines of the U.S. National Institutes of Health, the Academy of Sciences of the Czech Republic, and the human studies approving officials of the U.S. EPA. Group 1 samples were collected from November 17 – December 6, 2004. All of these samples were fixed immediately in formalin (3 days) and transferred to 4% paraformaldehyde (24 h) before embedding in paraffin. Group 2 samples were collected from October 17, 2000 – January 26, 2001, immediately frozen, and stored frozen at −80°C for approximately 5 years, at which time the tissue was thawed, a portion was fixed according to the same protocol used with Group 1, and processed for paraffin embedding. DNA was extracted from additional thawed portions of the samples in Group 2 and analyzed for AB sites and stable/bulky DNA adducts. Placenta donors in Group 1 included 7 smokers and 7 non-smokers; Group 2 included 18 smokers and 19 non-smokers.

BPDE-DNA Antiserum

The antiserum used for these studies, rabbit #30 bleed 6/30/78, was elicited against DNA modified with r7, t8-dihydroxy-t-9, 10-oxy-7,8,9,10-tetrahydrobenzo[*a*]pyrene (BPDE) [Poirier et al., 1980; Weston et al., 1989] and has specificity for the different enantiomers of benzo[*a*]pyrene (BP) bound to DNA, but no specificity for BP alone, BP metabolites, BP bound to protein, or DNA alone [Poirier et al., 1980]. Cross-reactivity of this antiserum for DNA samples modified with a series of carcinogenic PAHs has been reported [Weston et al., 1989]; therefore, when using human samples, which are likely to contain DNA adducts of multiple PAHs, the values obtained are designated PAH-DNA adducts.

BPDE-DNA Chemiluminescence Immunoassay (CIA)

The microtiter plate immunoassay for quantifying r7, t8, t9-trihydroxy-c-10-(N^2deoxyguanosyl)-7, 8, 9, 10-tetrahydro-benzo[*a*]pyrene (BPdG) adducts by CIA has been reported in detail [Divi et al., 2002]. For this study the standard curve 50% inhibition was 0.25 ± 0.05 fmol/well (mean ± SD) BPdG adducts (n = 5), and using 50 ng DNA per well, the lower limit of detection was 26 BPdG adducts/10^8 nucleotides.

IHC with the BPDE-DNA antiserum

To achieve lower backgrounds in the IHC staining, all antiserum was pre-absorbed with DNA before use. In addition, to prepare immunogen-absorbed BPDE-DNA antiserum from which the specific anti-BPDE-DNA antibodies have been removed, 0.05 ml of BPDE-DNA antiserum was absorbed two times with a total of 390 μg BPDE-DNA (1.3% modified, 13.9 nmol BPDE-DNA adducts). Antigen-antibody complexes were pelleted by centrifugation, and the final supernatant was used for staining.

Immunohistochemical staining of human tissues with the anti-BPDE-DNA antiserum has been described previously [Pratt et al., 2007; van Gijssel et al., 2002; van Gijssel et al., 2004]. In these experiments three serial 5-μm sections, designated a, b, and c, were cut from each paraffin block and stained within 3 weeks. Section b was stained with hematoxylin and used to obtain an accurate count of all nuclei in each region of interest. Sections a and c were stained with either BPDE-DNA antiserum or with immunogen-absorbed BPDE-DNA antiserum, both diluted 1:20,000. Fresh-cut sections were prepared, and staining was performed using the Nexes IHC (Ventana Medical Systems, Tucson, AZ) automated slide staining system essentially as described [Pratt et al., 2007]. The system was set for a 20-min incubation of the primary antiserum or immunogen-absorbed primary antiserum with no counterstaining. Section b for all tissues was stained for 8 min with hematoxylin (Ventana) followed by a 2-min incubation with bluing reagent (Ventana). Stained slides were rinsed in water containing Dawn dishwashing liquid soap (Proctor and Gamble, Cincinnati, OH) for 1 min, and subsequently rinsed in deionized water to remove the soap. Stained slides were air dried and mounted with Permount mounting medium (Fisher Scientific, Pittsburgh, PA).

Preparation of an IHC standard curve with BPDE-exposed cultured human cervical keratinocytes

Confluent normal human cervical keratinocytes immortalized with HPV16 (JCRB0140 [NCE16], Japan Health Sciences Foundation) were exposed to doses of 0, 0.053, 0.153, and 0.331 μM of BPDE for 1 h, as described [Pratt et al., 2007; van Gijssel et al., 2002]. Each group consisted of 15 identically treated 150 mm dishes. After cells were combined, centrifuged 5 min at 1000 rpm, and the supernatant removed, a portion of each resulting cell pellet was embedded in 3% SeaPlaque Agarose (Lonza, Basel, Switzerland), fixed in 10% buffered formalin (Sigma, St. Louis, MO), and embedded in paraffin. A second portion was extracted using an Intergen DNA extraction kit (Serologicals Corp., Norcross, GA) according to the instructions of the manufacturer. The DNA samples were analyzed by BPDE-DNA CIA in triplicate. The cells embedded in paraffin were used to generate arrays consisting of 3- × 1- mm cores of cell pellet for each of the three doses and control, resulting in a 3 × 4 “standard array” of cells treated with the incremental doses of BPDE. One standard array was stained along with each batch of samples. Data obtained for BPdG adduct levels in the human keratinocytes by BPDE-DNA CIA were compared with IHC values determined by Automated Cellular Imaging System (described below) in the same cells, thus producing a standard curve that could be used to calculate semi-quantitative values for adducts/10^8 nucleotides in the biological samples.

Semi-quantitation of nuclear staining intensity by IHC/ACIS

The intensity of the nuclear PAH-DNA adduct staining (pink color) was determined from digital images collected and evaluated using the ACIS II (Clarient, Aliso Viejo, CA), essentially as described [Pratt et al., 2007; van Gijssel et al., 2002; van Gijssel et al., 2004]. The nuclei containing PAH-DNA adducts stained pink (hue = 222–237), and hematoxylin nuclear staining was blue (hue =141–227).

To quantify the PAH-DNA adduct staining, a high-resolution composite digital image of each section was constructed using the ACIS II microscope and software. Within each imaged section, areas of chorionic villi containing CT and ST cells were selected for analysis using the ACIS region selection tools. For quantifying adducts in a particular sample, at least three regions per section were selected, and the same regions were localized on the corresponding hematoxylin stained sections, where the total number of nuclei were counted manually. Typically, up to 200 nuclei were evaluated per section. For sections in which the selected regions displayed low or zero OD values, the scoring was halted after at least 100 nuclei had been evaluated over 4 or more regions. For each section, a mean OD/nucleus value was obtained by adding all the OD values and dividing that sum by the total number of hematoxylin-stained nuclei.

Detection of AB sites

AB sites were determined as described [Swartz et al., 2009]. Briefly, DNA was isolated from whole placenta using the PUREGENE DNA Purification Kit for 100–300 mg solid tissue (Qiagen Inc., Valencia, CA). The manufacturer’s protocol was modified to include the use of the antioxidant 2,2,6,6-tetramethyl-1-piperidinyloxy, which is a free-radical scavenger [McDorman et al., 2005]. AB sites in the isolated DNA were detected using the Bio Vision DNA Damage Quantification Kit (Bio Vision Research Products, Mountain View, CA, Cat. No. K253-25) [Xiao et al., 2008], which determines AB sites based on the binding of a probe to aldehydic sites that are present in AB regions of DNA.

^{32}P-postlabeling detection of stable/bulky DNA adducts

Stable/bulky, high molecular weight DNA adducts were detected using the ^{32}P-postlabeling assay as described [King et al., 1994; King et al., 2001; Weyand et al., 1987]. This assay detects groups of spots by thin-layer chromatography and further purifies these on HPLC. We found that adducts in human samples determined by this assay were not chemically identifiable but were considered to include PAH-DNA adducts. Each DNA (50 μg) sample was digested with a mixture of micrococcal endonuclease and spleen phosphodiesterase for 3.5 h at 37°C. DNA adducts were enriched by butanol extraction and evaporated to dryness *in vacuo*. Samples were incubated with 50 μCi of [γ-^{32}P]ATP (>3000 Ci/mmol) and 3.5 U of T_4 polynucleotide kinase for 30 min at 37°C, and total incubates were applied to polyethyleneimine (PEI)-cellulose thin-layer chromatography (TLC) plates. Labeled DNA digests were spotted on 10 cm × 10 cm PEI-cellulose sheets and separated using a TLC system (D1 direction only). Following autoradiography to locate spots, samples were prepared for HPLC analyses [King et al., 1994; King et al., 2001; Weyand et al., 1987]. Major PEI-cellulose adduct spots (1 cm^2) were cut out and placed in scintillation vials containing 5 ml of ethanol to determine total radioactivity. Ethanol was decanted after counting, and adducted spots were extracted overnight (18 h) in 1 ml of 4-M pyridinium formate (pH 4). Extracts were transferred to 1.5 ml microcentrifuge vials, and particulate material was sedimented by centrifugation (10,000 rpm, 1 min). Total radioactivity (DPM) in the 4-M pyridinium formate extracts was determined, and sample volumes were reduced to dryness *in vacuo*, resuspended with 100 μl of a 9:1 mixture of methanol:0.3 M sodium phosphate buffer (pH 2.0), vortexed, and centrifuged again (10,000 rpm, 1 min). Supernatant (75 μl) from each sample was carefully removed and spiked with 4 nmol (8 μl) of the UV marker, *cis*-9,10-dihydroxy-9,10-dihydrophenanthrene. Volumes were adjusted to 100 μl with a 9:1 mixture of MeOH: 0.3 M NaH_2PO_4 buffer (pH 2) and placed in 100 μl autosampler vials for HPLC analysis.

We separated ^{32}P-labeled nucleoside-3',5'-bisphosphate adducts on a Hewlett-Packard Series 1100 HPLC System (Hewlett-Packard Company, Wilmington, DE) using a 5-μm, 4.6-mm × 250-mm Zorbax phenyl-modified column (MAC-MOD Analytical, Inc., Chadds Ford, PA). Adducted nucleotides were separated using a gradient elution consisting of the following solvent system: Solvent A: 0.5 M NaH_2HPO_4 buffer (pH 2.0); Solvent B: 90% methanol and 10% solvent A. The gradient was 0 to 12.5 min, 10 to 43% B; 12.5 to 60 min, 43 to 47% B; 60 to 83 min, 47 to 90% B; 83 to 90 min, 10% B. Flow rate was 1 ml/min, and the column was allowed to equilibrate at the initial solvent ratio (90% A: 10% B) for 15 min before subsequent analysis. Radiolabeled nucleotides were detected by an in-line flow-through scintillation counter (Model A-500 Flow-One\β Radiomatic Instruments & Chemical Co., Inc., Tampa, FL). The retention times of ^{32}P-postlabeled DNA adducts were expressed as relative retention time (RRT), calculated by dividing the retention time of the ^{32}P-postlabeled DNA adducts by the retention time of the internal UV standard (*cis*-9,10-dihydroxy-9,10-dihydrophenanthrene).

The procedure used to estimate the adduct level was a published modification [King et al., 1999] of the procedure of Gorelick et al. [Gorelick and Wogan, 1989]. Adduct-associated radioactivity in each HPLC run was calculated using the following equation:

$$\text{Adduct}-\text{associated } ^{32}\text{P (fmole)} = \frac{\text{DPM}}{(\text{SA})\,(\text{D})}$$

Where: DPM = DPM in nucleotide adduct peak; D = decay of [^{32}P]; SA = specific activity of [γ-^{32}P] ATP (6660 DPM /fmole). Conversion between molar amounts of adducts and DNA modification level was accomplished using an average molecular weight of

nucleotides (324 per nucleotide) to express a molar ratio of adducts to nucleotides in DNA. The binding levels were determined using the following equation:

$$\text{Binding level (adducts/fmole)} = \frac{\text{Adduct-associated } ^{32}\text{P (fmole)}}{\text{DNA per sample (fmole)}}$$

Statistical methods

AB site data were analyzed by one-way ANOVA with a Tukey-Kramer Multiple Comparisons Test using GraphPad Instat Version 3.06, 32 bit for Windows (GraphPad Software, San Diego, CA). The mathematical relationship and correlation between the BPDE-DNA IHC/ACIS values and BPDE-DNA CIA determinations of the BPDE-exposed human cervical keratinocytes was determined using the method of least squares. We tested for statistical differences in median PAH-DNA adduct levels and AB sites between smokers and non-smokers and exposure to ETS using the Mann-Whitney test. Comparisons of DNA adduct levels as determined by the different methods were performed using the Spearman correlation.

Results

BPDE standard curve using human keratinocytes

Cultured human cervical keratinocytes were exposed to 0, 0.053, 0.153, or 0.331 μM of BPDE, and using the BPDE-DNA antiserum, values for IHC staining determined by ACIS were compared to BPdG values determined by CIA using the same samples. Fig. 1A shows a representative IHC/ACIS dose-response for BPdG adduct formation (pink staining) in keratinocyte nuclei, with the doses of BPDE used and the resulting ACIS-derived color intensity values (optical density [OD]/nucleus). The low background, 42 OD/nucleus seen for unexposed cells, was used as a correction factor for values obtained with the BPDE doses. For adduct determination, the IHC standard curve was normalized so that the highest linear value, the color intensity obtained at 0.153-μM BPDE, was expressed as 100%; this was considered appropriate as color intensity for all of the unknown samples fell below this value.

A composite normalized IHC/ACIS standard curve that includes values for 6 different stainings is shown in Fig. 2 (ordinate). Fig. 2 (abscissa) shows mean BPdG values determined by BPDE-DNA CIA for the 0, 0.053, and 0.153-μM BPDE doses, which were 0, 114.7 ± 26.0, and 362.4 ± 23.9 (mean ± SD, n = 3/group) adducts/10^8 nucleotides, respectively. Fig. 2, a composite plot of all these analyses, shows a strong linear relationship between the mean BPdG values determined by IHC/ACIS (n = 6) and those determined by BPDE-DNA CIA (n = 5) ($R^2 = 0.99$), and functions as a standard curve to provide a semi-quantitative estimation of PAH-DNA adducts for the samples in question.

IHC determination of PAH-DNA adducts in human placenta: Group 1

In 2004 in Teplice, the Group 1 placenta samples were collected at delivery from 14 women, and the tissue was fixed immediately in formalin and embedded in paraffin. In our laboratory, serial sections from each paraffin block were stained with specific BPDE-DNA antiserum, immunogen-absorbed BPDE-DNA antiserum, or hematoxylin. Fig. 1B shows two representative samples from Group 1 (4152 in i, ii and iii; and 4157 in iv, v and vi), in which the cells chosen for ACIS analysis are outlined in blue. Panels (i) and (iv) show blue hematoxylin staining, and panels (ii) and (v) show the same outlined areas stained with specific BPDE-DNA antiserum where pink nuclei indicate the presence of PAH-DNA adducts. Fig. 1B, panels (iii) and (vi) show staining with the immunogen-absorbed BPDE-

DNA antiserum where a virtually complete loss of pink nuclear intensity confirms that the PAH-DNA staining is specific. Insets in Fig. 1B (ii), (iii), (v) and (vi) show OD/nucleus values for color intensity.

Color intensity values for staining of Group 1 samples with specific BPDE-DNA antiserum, including 7 smokers (S, ■), 7 non-smokers (NS, □), and replicates of the 0.153-μM BPDE standard curve dose (▨) are shown in Fig. 3. Fig. 3 also shows the same samples stained with absorbed (▩) BPDE-DNA antiserum. The color intensity for the sections stained with absorbed serum (4 – 599 OD/nucleus) was minor when compared to the staining values with the BPDE-DNA antiserum, which ranged from 1,822 to 11,641 OD/nucleus. The substantial reduction of pink staining in all samples incubated with absorbed antiserum, compared to those incubated with specific antiserum, indicates that the staining in the placenta samples is specific for PAH-DNA adducts.

Human cervical keratinocyte standard curves (see composite Fig. 2) were used to estimate the quantity of PAH-DNA adducts in the human placenta specimens. The specific antiserum OD/nucleus values, corrected for the absorbed-serum background and normalized based on the standard curve generated for that particular staining, were read against the composite standard curve. For the Group 1 samples the IHC/ACIS values ranged from 49 to 312 PAH-DNA adducts/10^8 nucleotides (Table I), well above the lower limit of detection (0.2 adducts/10^8 nucleotides). Table I shows the samples, grouped by smoking status of the mother, the number of nuclei examined, and the mean and median PAH-DNA adduct values, which were essentially the same in the smoking and non-smoking groups. Table I also shows the ETS status of each mother during her pregnancy, and it is interesting to note that all women, except for 2 non-smokers, were exposed to tobacco smoke in their ambient environment. The median and interquartile ranges for PAH-DNA adducts/10^8 nucleotides in the 7 smokers and the 7 non-smokers are shown in the Table and were not significantly different (Mann-Whitney, p= 0.7).

IHC determination of PAH-DNA adducts in human placenta: Group 2

The Group 2 samples, collected from 37 women in the Teplice region in 2000 and 2001, were initially frozen, and portions of tissue were thawed to extract DNA that was used for AB site and ^{32}P-postlabeling evaluations. In 2006 additional frozen tissue was thawed, fixed and embedded in paraffin, and serial sections from each sample were stained with specific BPDE-DNA antiserum, immunogen-absorbed BPDE-DNA antiserum, or hematoxylin. Staining was evaluated in 100 to 224 nuclei per section, and using the standard curve to calculate PAH-DNA adducts/10^8 nucleotides, values ranged between non-detectable and 5.6 adducts/10^8 nucleotides (Fig. 4A). Because most of the PAH-DNA adduct values in Group 2 were below the limit of detection (0.01 adducts/10^8 nucleotides), while the standard curve staining intensity was similar for both Group 1 and Group 2 samples, we suspected degradation in the Group 2 placentas. When a sample from Group 1 was stained simultaneously with a sample from Group 2, the Group 2 sample had a much lower signal (see Fig. 1C panels (i) and (ii), respectively). We therefore hypothesized that freezing the samples resulted in tissue degradation that was evidenced by loss of IHC staining intensity. This hypothesis was addressed in the next experiment.

Comparison of PAH-DNA adducts determined by IHC/ACIS in frozen vs. fresh-fixed tissue

To determine whether or not initial freezing altered the detectability of BPdG adducts, human cervical keratinocytes, at 80% confluency, were exposed for 1 h to 4.0-μM BPDE, and the resulting cell pellet was split into two equal portions. One portion was fixed immediately in 10% buffered formalin for 24 h before paraffin embedding. The second portion was frozen at −80°C for 45 days, thawed briefly, then fixed and embedded. The

resulting staining intensity for both the frozen and freshly fixed cell pellets is shown in Fig. 5. The sample that was frozen before fixation had an intensity of 17,836 ± 3,217 OD/nucleus (mean ± SE, n = 5 regions, 137 cells), which was significantly less than the 23,823 ± 3,605 OD/nucleus (mean ± SE, n = 5 regions, 136 cells) observed for the freshly fixed cells (p= 0.03, paired t test). Therefore, because freezing for 45 days, followed by routine fixation and embedding, was sufficient to reduce the BPdG adduct signal in cultured cells by 25%, it is likely that freezing the placenta samples for several years resulted in tissue degradation and loss of IHC staining.

DNA damage in Group 2 samples determined by ^{32}P-postlabeling and AB sites

Evaluation of stable/bulky DNA adduct levels using ^{32}P-postlabeling, and measurement of AB sites, were performed using DNA extracted from the Group 2 samples (n = 37), and the data are shown in Table II for smokers and non-smokers. In addition, in Fig. 4 samples are grouped as smokers (■, n = 18), non-smokers with environmental tobacco smoke (ETS) exposure (□, n = 9) and non-smokers with no ETS (▩, n = 10). A comparison of smokers and non-smokers for the ^{32}P-postlabeling analysis (see Table II) revealed 5.0 ± 2.0 adducts/10^8 nucleotides (mean ± SD) among the smokers (n = 18) and 4.8 ± 1.7 adducts/10^8 nucleotides (mean ± SD) for the non-smokers (n = 19). There was also no significant difference in adduct levels between women who were either smokers or exposed to ETS (n = 27) and women exposed to neither (n = 10) (p = 0.13).

Table II and Fig. 4C show values for AB sites. Again, there was no difference in the number of AB sites observed in smokers (12.5 ± 8.5 sites/10^5 nucleotides) compared to non-smokers (13.3 ± 12.2 sites/10^5 nucleotides) (p= 0.6), or between women who smoked or were exposed to ETS (13.1 ± 9.9 sites/10^5 nucleotides, n = 27) when compared to women who neither smoked nor were exposed to ETS (12.4 ± 3.9 sites/10^5 nucleotides, n = 10) (p= 0.2).

Discussion

The placentas examined in this study were obtained from mothers living in the Czech mining district of Teplice, an area which, 30 years ago, was considered to have some of the worst environmental pollution in Europe. In the intervening time the environment has improved, but Teplice continues to have high levels of pollution. This study was designed to examine different classes of DNA damage, including PAH-DNA adducts determined by IHC/ACIS, stable/bulky DNA adducts determined by ^{32}P- postlabelling and unstable AB sites detected by specific probe. All 3 types of DNA damage were found in Teplice placenta samples; however, due to technical difficulties, we were not able to examine all 3 biomarkers in each single placenta. The exposures that resulted in these varied types of DNA damage are likely complex. However, we conclude that these placentas, taken from a polluted region of the Czech Republic, sustained substantial genotoxic damage in the form of both stable and unstable DNA adducts.

An important novel finding of this study is the localization of PAH-DNA adducts by IHC BPDE-DNA staining with ACIS analysis of color intensity. The data confirmed a suspected concentration of PAH-DNA adducts in the metabolically active CT cells and ST knots, which line the external surface of the chorionic villi and are bathed in the maternal blood supply. The purpose of these cells is to protect the infant from xenobiotics, and given the level of DNA damage that they sustain, the system appears to work well. The PAH-DNA adduct values generated by the semi-quantitative standard curve are relatively high, but perhaps not unexpected because only the ST and CT cells were examined for the IHC measurements. In this and other studies involving human cervix, prostate, and esophagus [John et al., 2009; Pratt et al., 2007; van Gijssel et al., 2002; van Gijssel et al., 2004], we

have used a similar approach to demonstrate strong signals for PAH-DNA adduct formation, localized primarily in basal epithelium of the tissue in question. The consistency and ease of this staining provides a particularly robust approach for molecular epidemiology studies, and the adduct localization provides a powerful tool with which to elucidate tissue response to xenobiotic insult.

We found no correlations among the values obtained for the three types of DNA damage in human placenta. The lack of a correlation between stable/bulky DNA adducts and unstable AB sites likely reflects the fact that these methods detect structurally different types of DNA damage that may have been induced by different chemicals. Using the BPDE-DNA antiserum, IHC detects adducts of several carcinogenic PAHs [Weston et al., 1989]. In contrast, ^{32}P-postlabeling is presumed to detect some types of PAH-DNA damage that are not recognized by the BPDE-DNA antiserum. In addition, AB sites may be caused by a variety of types of agents, including alkylating agents and sulfur-PAH [Maynard et al., 2009; Swartz et al., 2009].

The loss of PAH-DNA adduct signal in placentas that were frozen before fixation, compared to fresh-fixed placentas, was unexpected. However, this effect was replicated in frozen and fresh-fixed cultured keratinocyte samples, and further confirmed with simultaneous re-staining of human placenta samples from Groups 1 and 2. The apparent loss of PAH-DNA adducts that occurred in frozen samples, which were subsequently paraffin-embedded, constitutes an important cautionary tale for molecular epidemiology studies. Although PAH-DNA adducts are stable for years in frozen tissues, we hypothesize that freezing and thawing compromise the tissue architecture, diminishing subsequent antigen retrieval.

It is likely that airborne PAHs are responsible primarily for the DNA damage observed in this study. However, a potentially-confounding source of PAH exposure is diet. Strong correlations have been reported between PAH-DNA adducts and the foods being consumed [Kang et al., 1995; Rothman et al., 1990], and diet is considered by some to be a major source of PAH exposure [Bostrom et al., 2002; Ramesh et al., 2004]. In the present study, dietary PAHs were not considered to be a primary source of exposure because the Czech diet, which rarely includes char-grilled meats, is quite different from that consumed by the U.S. population. Furthermore, extensive research in the Teplice region has suggested that 70–75% of carcinogenic PAH exposures come from air pollution [Sram, 2001].

Evaluation of smoking and non-smoking status did not reveal significant differences in level of placental DNA damage in smokers and non-smokers for any of the three biomarkers. However, only 12 of the 51 women studied reported no exposure to either ETS and/or cigarette smoking during their pregnancies. Using the BPDE-DNA antiserum, we and others have not found correlations between PAH-DNA adduct levels and smoking [Gyorffy et al., 2008; Pratt et al., 2007], although stable/bulky-DNA adducts determined by ^{32}P-postlabeling typically correlate with extent of tobacco smoke exposure [Phillips, 2002]. We have shown, using both assays, that leukocyte PAH-DNA adduct levels increased in a population moving from an area with low PAH exposure to an area with a more polluted environment [Poirier et al., 1998]. Therefore, the lack of a smoking correlation in the current study may indicate that additional sources of PAH exposure, including ETS and ambient pollution from industrial and/or indoor heating sources [Binkova et al., 2003], may be sufficiently high to dilute any smoking effect.

Multiple studies have reported adduct formation in DNA extracted from human placenta, and most of these have employed either ^{32}P-postlabeling [Marafie et al., 2000] or some form of Enzyme-linked Immunosorbent Assay with a BPDE-DNA antiserum [Arnould et al., 1997; Sanyal et al., 2007; Whyatt et al., 1998]. The values reported here for ^{32}P-postlabeling

are in the same range as those reported previously for non-smoking mothers in winter in Teplice ($1.5/10^8$ nucleotides) [Topinka et al., 1997] and non-smoking women in Kuwait and London ($2–4/10^8$ nucleotides) [Marafie et al., 2000]. Both of these studies showed significant increases in placental DNA adducts as determined by ^{32}P-postlabelling in women who smoked compared with women who did not smoke. PAH-DNA values determined by BPDE-DNA ELISA were not significantly higher in women who smoked, compared to women who did not smoke [Arnould et al., 1997; Sanyal et al., 2007; Whyatt et al., 1998]. However, the PAH-DNA adduct values appeared higher than the adduct levels determined by ^{32}P-postlabelling in two studies where whole placenta was used (6.5–8.5 adducts/10^8 nucleotides) [Sanyal et al., 2007; Whyatt et al., 1998], and in one study where syncytial nuclei were concentrated and used for analysis (7–40 adducts/10^8 nucleotides) [Arnould et al., 1997]. The study presented here shows that the levels of DNA adducts determined by ^{32}P-postlabelling are similar to literature values. In addition, the localization of PAH-DNA adducts in ST and CT cells suggest that DNA damage induced by other xenobiotic agents may also localize in these cells as a result of their metabolic competence. Therefore, it may be of value in future studies of human placental DNA to concentrate ST and CT nuclei prior to DNA extraction, as described [Manchester et al., 1988] and used [Arnould et al., 1997] previously.

In conclusion, in this study we examined 51 placentas obtained from mothers living in the highly polluted Czech mining district of Teplice. We found evidence for multiple types of DNA damage in all of the placentas. These included PAH-DNA adducts, stable/bulky (considered largely hydrophobic) DNA adducts, and AB sites that result in DNA strand breaks. In addition, we observed that long-term freezing of a tissue, prior to fixation, paraffin-embedding, and staining, resulted in a significant loss in the PAH-DNA adduct signal. Overall, we conclude that these placentas, taken from a highly polluted region of the Czech Republic, sustained substantial genotoxic damage in the form of both stable and unstable DNA adducts.

Abbreviations

AB site	abasic site
ACIS	Automated Cellular Imaging System
BP	benzo[*a*]pyrene (CAS No. 50-32-8)
BPDE	r7, t8-dihydroxy-t-9, 10-oxy-7,8,9,10-tetrahydrobenzo[*a*]pyrene (CAS No. 58917-67-2)
BPdG	r7, t8, t9-trihydroxy-c-10-(N^2deoxyguanosyl)-7, 8, 9, 10-tetrahydro-benzo[*a*]pyrene
CIA	chemiluminescence immunoassay
CT	cytotrophoblast
ETS	environmental tobacco smoke
HPLC	High Pressure Liquid Chromatography
IHC	immunohistochemistry
IUGR	Intrauterine growth retardation
NS	non-smoker
OD	optical density, or mean color intensity reported by the ACIS
PAHs	polycyclic aromatic hydrocarbons

PEI	polyethyleneimine
S	smoker
ST	syncytiotrophoblast
TLC	Thin Layer Chromatography

Acknowledgments

This research was supported by the Intramural Research Program of the National Institutes of Health, National Cancer Institute, Center for Cancer Research, by the United States Environmental Protection Agency, and by the Czech Ministry of Environment SP/1b3/8/8/08. We thank J. Ross, S. Nesnow, and B. Collins for their helpful comments on this manuscript. This manuscript was pre-reviewed by the National Health and Environmental Effects Research Laboratory, U.S. Environmental Protection Agency, and National Cancer Institute, National Institutes of Health, and approved for publication. Approval does not signify that the contents necessarily reflect the views and policies of the Agency, nor does mention of trade names or commercial products constitute endorsement or recommendation for use.

REFERENCES

Arnould JP, Verhoest P, Bach V, Libert JP, Belegaud J. Detection of benzo[a]pyrene-DNA adducts in human placenta and umbilical cord blood. Hum Exp Toxicol. 1997; 16:716–721. [PubMed: 9429085]

Binkova B, Cerna M, Pastorkova A, Jelinek R, Benes I, Novak J, Sram RJ. Biological activities of organic compounds adsorbed onto ambient air particles: comparison between the cities of Teplice and Prague during the summer and winter seasons 2000–2001. Mutat Res. 2003; 525:43–59. [PubMed: 12650904]

Bostrom CE, Gerde P, Hanberg A, Jernstrom B, Johansson C, Kyrklund T, Rannug A, Tornqvist M, Victorin K, Westerholm R. Cancer risk assessment, indicators, and guidelines for polycyclic aromatic hydrocarbons in the ambient air. Environ Health Perspect. 2002; 110:451–488. [PubMed: 12060843]

Cross JC, Nakano H, Natale DR, Simmons DG, Watson ED. Branching morphogenesis during development of placental villi. Differentiation. 2006; 74:393–401. [PubMed: 16916377]

Dejmek J. The impact of polycyclic aromatic hydrocarbons and fine particles on pregnancy outcome. Environ Health Perspect. 2000; 108:1159–1164. [PubMed: 11133396]

Dejmek J, Selevan SG, Benes I, Solansky I, Sram RJ. Fetal growth and maternal exposure to particulate matter during pregnancy. Environ Health Perspect. 1999; 107:475–480. [PubMed: 10339448]

Divi RL, Beland FA, Fu PP, Von Tungeln LS, Schoket B, Camara JE, Ghei M, Rothman N, Sinha R, Poirier MC. Highly sensitive chemiluminescence immunoassay for benzo[*a*]pyrene-DNA adducts: validation by comparison with other methods, and use in human biomonitoring. Carcinogenesis. 2002; 23:2043–2049. [PubMed: 12507927]

Gorelick NJ, Wogan GN. Fluoranthene-DNA adducts: identification and quantification by an HPLC-32P-postlabeling method. Carcinogenesis. 1989; 10:1567–1577. [PubMed: 2670301]

Gyorffy E, Anna L, Kovacs K, Rudnai P, Schoket B. Correlation between biomarkers of human exposure to genotoxins with focus on carcinogen-DNA adducts. Mutagenesis. 2008; 23:1–18. [PubMed: 17989146]

John K, Ragavan N, Pratt MM, Singh PB, Al-Buheissi S, Matanhelia SS, Phillips DH, Poirier MC, Martin FL. Quantification of phase I/II metabolizing enzyme gene expression and polycyclic aromatic hydrocarbon-DNA adduct levels in human prostate. The Prostate. 2009; 69:505–519. [PubMed: 19143007]

Kang DH, Rothman N, Poirier MC, Greenberg A, Hsu CH, Schwartz BS, Baser ME, Groopman JD, Weston A, Strickland PT. Interindividual differences in the concentration of 1-hydroxypyrene-glucuronide in urine and polycyclic aromatic hydrocarbon-DNA adducts in peripheral white blood

cells after charbroiled beef consumption. Carcinogenesis. 1995; 16:1079–1085. [PubMed: 7767968]

King LC, Adams L, Allison J, Kohan MJ, Nelson G, Desai D, Amin S, Ross JA. A quantitative comparison of dibenzo[a,l]pyrene-DNA adduct formation by recombinant human cytochrome P450 microsomes. Mol Carcinog. 1999; 26:74–82. [PubMed: 10506751]

King LC, George M, Gallagher JE, Lewtas J. Separation of 32P-postlabeled DNA adducts of polycyclic aromatic hydrocarbons and nitrated polycyclic aromatic hydrocarbons by HPLC. Chem Res Toxicol. 1994; 7:503–510. [PubMed: 7526903]

King LC, Kohan MJ, Brooks L, Nelson GB, Ross JA, Allison J, Adams L, Desai D, Amin S, Padgett W, Lambert GR, Richard AM, Nesnow S. An evaluation of the mutagenicity, metabolism, and DNA adduct formation of 5-nitrobenzo[b]naphtho[2,1-d]thiophene. Chem Res Toxicol. 2001; 14:661–671. [PubMed: 11409936]

Lewtas J. Air pollution combustion emissions: Characterization of causative agents and mechanisms associated with cancer, reproductive, and cardiovascular effects. Mutat Res. 2007; 636:95–133. [PubMed: 17951105]

Manchester DK, Weston A, Choi JS, Trivers GE, Fennessey PV, Quintana E, Farmer PB, Mann DL, Harris CC. Detection of benzo[a]pyrene diol epoxide-DNA adducts in human placenta. Proc Natl Acad Sci U S A. 1988; 85:9243–9247. [PubMed: 3143115]

Marafie EM, Marafie I, Emery SJ, Waters R, Jones NJ. Biomonitoring the human population exposed to pollution from the oil fires in Kuwait: Analysis of placental tissue using P-32-postlabeling. Environ Mol Mutagen. 2000; 36:274–282. [PubMed: 11152560]

Maynard S, Schurman SH, Harboe C, de Souza-Pinto NC, Bohr VA. Base excision repair of oxidative DNA damage and association with cancer and aging. Carcinogenesis. 2009; 30:2–10. [PubMed: 18978338]

McDorman KS, Pachkowski BF, Nakamura J, Wolf DC, Swenberg JA. Oxidative DNA damage from potassium bromate exposure in Long-Evans rats is not enhanced by a mixture of drinking water disinfection by-products. Chem Biol Interact. 2005; 152:107–117. [PubMed: 15840384]

Phillips DH. Smoking-related DNA and protein adducts in human tissues. Carcinogenesis. 2002; 23:1979–2004. [PubMed: 12507921]

Poirier MC, Santella R, Weinstein IB, Grunberger D, Yuspa SH. Quantitation of benzo(a)pyrene-deoxyguanosine adducts by radioimmunoassay. Cancer Res. 1980; 40:412–416. [PubMed: 7356524]

Poirier MC, Weston A, Schoket B, Shamkhani H, Pan CF, McDiarmid MA, Scott BG, Deeter DP, Heller JM, Jacobson-Kram D, Rothman N. Biomonitoring of United States Army soldiers serving in Kuwait in 1991. Cancer Epidemiol Biomarkers Prev. 1998; 7:545–551. [PubMed: 9641500]

Pratt MM, Sirajuddin P, Poirier MC, Schiffman M, Glass AG, Scott DR, Rush BB, Olivero OA, Castle PE. Polycyclic aromatic hydrocarbon-DNA adducts in cervix of women infected with carcinogenic human papillomavirus types: An immunohistochemistry study. Mutat Res. 2007; 624:114–123. [PubMed: 17583755]

Ramesh A, Walker SA, Hood DB, Guillen MD, Schneider K, Weyand EH. Bioavailability and risk assessment of orally ingested polycyclic aromatic hydrocarbons. Int J Toxicol. 2004; 23:301–333. [PubMed: 15513831]

Rothman N, Correa-Villasenor A, Ford DP, Poirier MC, Haas R, Hansen JA, O'Toole T, Strickland PT. Contribution of occupation and diet to white blood cell polycyclic aromatic hydrocarbon-DNA adducts in wildland firefighters. Cancer Epidemiol Biomarkers Prev. 1993a; 2:341–347. [PubMed: 8348057]

Rothman N, Poirier MC, Baser ME, Hansen JA, Gentile C, Bowman ED, Strickland PT. Formation of polycyclic aromatic hydrocarbon-DNA adducts in peripheral white blood cells during consumption of charcoal-broiled beef. Carcinogenesis. 1990; 11:1241–1243. [PubMed: 2372884]

Rothman N, Poirier MC, Haas RA, Correa-Villasenor A, Ford P, Hansen JA, O'Toole T, Strickland PT. Association of PAH-DNA adducts in peripheral white blood cells with dietary exposure to polyaromatic hydrocarbons. Environ Health Perspect. 1993b; 99:265–267. [PubMed: 8319640]

Sanyal MK, Mercan D, Belanger K, Santella RM. DNA adducts in human placenta exposed to ambient environment and passive cigarette smoke during pregnancy. Birth Defects Res Part A Clin Mol Teratol. 2007; 79:289–294. [PubMed: 17286299]

Sram, RJ. Teplice Program: Impact of air pollution on human health. Prague: Academia; 2001. p. 1-318.

Sram RJ, Binkova B, Rossner P, Rubes J, Topinka J, Dejmek J. Adverse reproductive outcomes from exposure to environmental mutagens. Mutat Res. 1999; 428:203–215. [PubMed: 10517994]

Swartz CD, King LC, Nesnow S, Umbach DM, Kumar S, Demarini DM. Mutagenicity, stable DNA adducts, and abasic sites induced in Salmonella by phenanthro[3,4-b]- and phenanthro[4,3-b]thiophenes, sulfur analogs of benzo[c]phenanthrene. Mutat Res. 2009; 661:47–56. [PubMed: 19041882]

Topinka J, Binkova B, Mrackova G, Stavkova Z, Benes I, Dejmek J, Lenicek J, Sram RJ. DNA adducts in human placenta as related to air pollution and to GSTM1 genotype. Mutat Res. 1997; 390:59–68. [PubMed: 9150753]

van Gijssel HE, Divi RL, Olivero OA, Roth MJ, Wang GQ, Dawsey SM, Albert PS, Qiao YL, Taylor PR, Dong ZW, Schrager JA, Kleiner DE, Poirier MC. Semiquantitation of polycyclic aromatic hydrocarbon-DNA adducts in human esophagus by immunohistochemistry and the automated cellular imaging system. Cancer Epidemiol Biomarkers Prev. 2002; 11:1622–1629. [PubMed: 12496053]

van Gijssel HE, Schild LJ, Watt DL, Roth MJ, Wang GQ, Dawsey SM, Albert PS, Qiao YL, Taylor PR, Dong ZW, Poirier MC. Polycyclic aromatic hydrocarbon-DNA adducts determined by semiquantitative immunohistochemistry in human esophageal biopsies taken in 1985. Mutat Res. 2004; 547:55–62. [PubMed: 15013699]

Weston A, Manchester DK, Poirier MC, Choi JS, Trivers GE, Mann DL, Harris CC. Derivative fluorescence spectral analysis of polycyclic aromatic hydrocarbon-DNA adducts in human placenta. Chem Res Toxicol. 1989; 2:104–108. [PubMed: 2519708]

Weyand EH, Rice JE, LaVoie EJ. 32P-postlabeling analysis of DNA adducts from non-alternant PAH using thin-layer and high performance liquid chromatography. Cancer Lett. 1987; 37:257–266. [PubMed: 3677058]

Whyatt RM, Bell DA, Jedrychowski W, Santella RM, Garte SJ, Cosma G, Manchester DK, Young TL, Cooper TB, Ottman R, Perera FP. Polycyclic aromatic hydrocarbon- DNA adducts in human placenta and modulation by CYP1A1 induction and genotype. Carcinogenesis. 1998; 19:1389–1392. [PubMed: 9744534]

Xiao R, Su Y, Simmen RC, Simmen FA. Dietary soy protein inhibits DNA damage and cell survival of colon epithelial cells through attenuated expression of fatty acid synthase. Am J Physiol Gastrointest Liver Physiol. 2008; 294:G868–G876. [PubMed: 18239060]

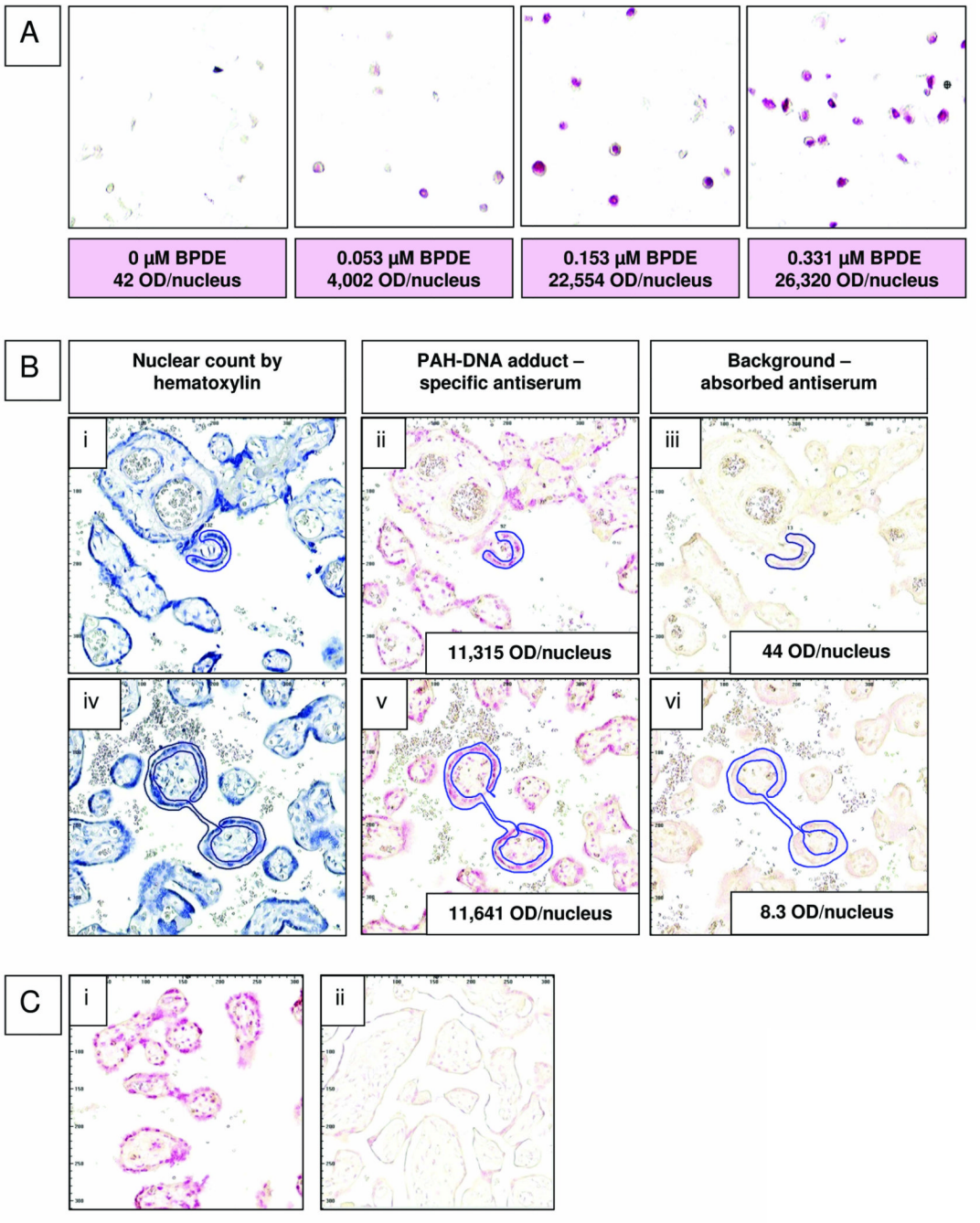

Fig. 1.

(A) Cultured human cervical keratinocytes exposed to 0, 0.053, 0.153, or 0.331-µM BPDE for 1 h were fixed, paraffin-embedded, and stained with rabbit anti-BPDE-DNA and Fast Red. Values for pink color intensity, optical density (OD)/nucleus, determined by ACIS are shown below each image. **(B)** Sequential sections from 2 human placenta samples were stained with either hematoxylin (i and iv), anti-BPDE-DNA antiserum (1:20,000, ii and v), or immunogen-absorbed anti-BPDE-DNA (1:20,000, iii and vi). Nuclei located in the regions designated for adduct analysis (outlined in blue with the ACIS regional selection tool) were counted on hematoxylin-stained slides. **(C)** Human placenta samples that were either fixed when fresh (Group 1, i), or frozen for 5 years before fixation (Group 2, ii) were

stained simultaneously with anti-BPDE-DNA (1:10,000); PAH-DNA adducts were virtually undetectable in the frozen samples.

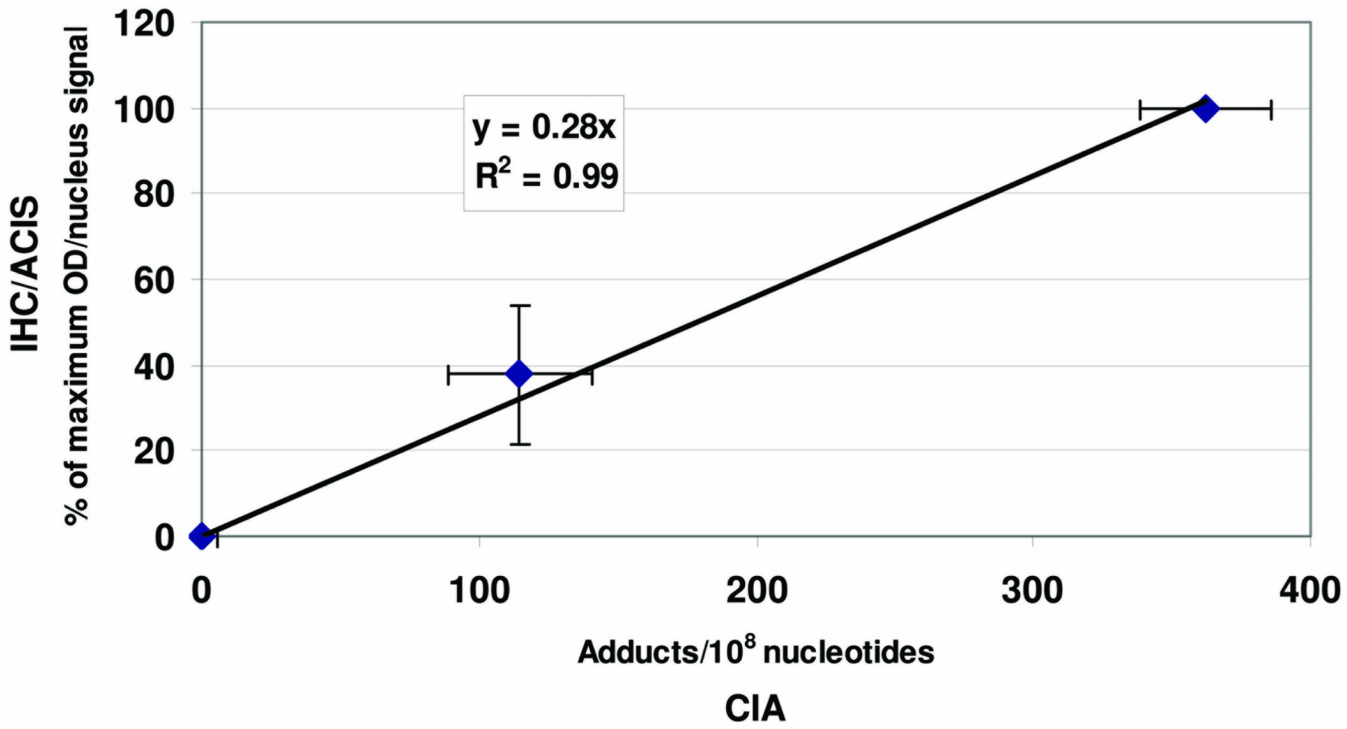

Fig. 2.

Cultured human cervical keratinocytes exposed to 0, 0.053, and 0.153-μM BPDE (see Fig. 1 A), were fixed, paraffin-embedded, analyzed by IHC/ACIS on ≥ 3 separate occasions, and plotted on the ordinate as % of Maximum OD/nucleus (mean ± SD), where 100% = the value obtained with 0.153 μM BPDE. A second aliquot of cells treated simultaneously was subjected to DNA extraction, BPdG adducts were measured 5 times by quantitative BPDE-DNA CIA, and data were plotted on the abscissa as BPdG adducts/10^8 nucleotides (mean ± SD). The correlation for the two adduct assays showed an R^2 of 0.99.

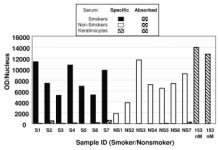

Fig. 3.

IHC staining with ACIS analysis of Group 1 human placentas showing OD/nucleus values for smokers (■, n = 7) and non-smokers (□, n = 7) using specific BPDE-DNA 27 antiserum, and absorbed BPDE-DNA antiserum (▩). The graph also shows values for human keratinocytes exposed to 0.153-μM BPDE and stained simultaneously (with the placentas) using specific (▨) or absorbed (▩) BPDE-DNA antiserum.

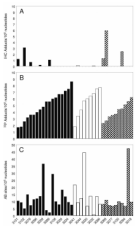

Fig. 4.

DNA damage in Group 2 placentas determined by (A) IHC, (B) ^{32}P-postlabeling and (C) AB site analysis. Samples are in the same order in each frame and grouped as: smokers (■); non-smokers with ETS exposure (□); and, non-smokers without ETS exposure (▩).

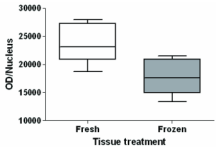

Fig. 5.

BPdG adducts in keratinocytes exposed to 4.0 μM BPDE for 1 h. One portion of the cell pellet was fixed and paraffin-embedded immediately after harvest, and the median value was 23,823 ± 3,605 OD/nucleus (n = 137 fresh nuclei). The rest of the cell pellet was frozen for 6 weeks, then fixed and paraffin embedded, and the median value was 17,836 ± 3,217 OD/nucleus (n = 137 frozen nuclei). The frozen cells had significantly-less BPdG adducts (OD/nucleus) than fresh-fixed cells (p= 0.03, one-tailed paired t-test, n = 5 regions/section).

TABLE I

PAH-DNA adducts determined by IHC/ACIS in Group 1 placentas stratified by smoking status.

Smokers				Non-Smokers			
Specimen	**Counted Nuclei**	**Adducts/ 10^8 nucleotides[a]**	**ETS[b]**	**Specimen**	**Counted Nuclei**	**Adducts/ 10^8 nucleotides[a]**	**ETS[b]**
4153	248	302.6	+	4152	197	48.8	+
4154	198	184.9	+	4156	203	103.0	+
4155	208	138.3	+	4157	215	312.3	+
4159	191	285.3	+	4158	203	190.3	−
4162	205	184.2	+	4160	206	171.9	+
4164	221	135.7	+	4161	202	196.5	+
4166	287	245.7	+	4163	283	237.8	−
Mean[c]		211.0 ± 25.6		Mean[c]		180.1 ± 32.5	
Median[d]		184.9 (138.3–285.3)		Median[d]		190.3 (103.0–237.8)	

[a] Limit of detection = 0.2 adducts/10^8 nucleotides

[b] Environmental tobacco smoke (ETS) exposure, + = yes, − = no

[c] Mean ± SE

[d] Median (25–75 percentile); Smokers vs. Nonsmokers, $p = 0.7$, Mann Whitney

TABLE II

Comparison of DNA damage in Group 2 human placenta determined by IHC, ^{32}P-postlabeling and abasic site analysis

ID	IHC Total Nuclei Counted	IHC/ACIS Adducts/ 10^8 Nucleotides	^{32}P-Postlabeling Adducts/ 10^8 Nucleotides	Abasic sites/ 10^5 Nucleotides[c]	ETS[b] Exposure
Smokers					
3019	110	_[a]	6.7	7.95 ± 0.42	+
3026	165	_[a]	6.7	18.27 ± 0.08	+
3027	143	_[a]	7.2	13.63 ± 0.32	+
3034	101	_[a]	7.5	9.62 ± 0.22	+
3040	116	_[a]	8.6	7.70 ± 0.12	+
3043	108	_[a]	1.8	9.43 ± 0.03	+
3049	107	_[a]	3.2	15.02 ± 0.43	+
3059	104	_[a]	4.8	36.63 ± 0.45	+
3061	103	0.23	4.4	13.78 ± 0.64	+
3078	105	0.72	3.6	7.42 ± 0.36	+
3082	126	_[a]	3.6	11.60 ± 0.33	+
3084	113	_[a]	6.0	29.43 ± 1.18	+
3086	105	_[a]	5.6	3.90 ± 0.35	+
3089	219	1.10	5.6	2.32 ± 0.16	+
3096	216	_[a]	4.0	12.13 ± 0.95	+
3101	209	1.21	1.7	10.60 ± 1.15	+
3102	223	3.14	2.6	5.15 ± 0.17	+
3108	224	_[a]	6.2	10.13 ± 0.08	+
Non-Smokers					
3017	198	_[a]	5.7	44.35 ± 1.0	+
3020	114	_[a]	6.0	6.63 ± 0.40	+
3024	103	_[a]	6.4	13.67 ± 0.27	+
3032	141	0.09	6.8	0.58 ± 0.12	+

ID	IHC Total Nuclei Counted	IHC/ACIS Adducts/ 10^8 Nucleotides	^{32}P-Postlabeling Adducts/ 10^8 Nucleotides	Abasic sites/ 10^5 Nucleotides[c]	ETS[b] Exposure
3038	111	_[a]	7.5	13.53 ± 0.70	+
3041	108	_[a]	1.8	21.70 ± 1.06	+
3044	118	_[a]	4.3	12.15 ± 1.13	+
3066	114	_[a]	7.7	7.95 ± 0.23	+
3103	203	0.15	3.4	9.07 ± 0.82	+
3018	114	_[a]	6.2	9.55 ± 0.53	−
3060	194	_[a]	5.6	47.15 ± 0.93	−
3068	216	5.91	2.7	10.93 ± 0.75	−
3076	112	_[a]	3.3	7.22 ± 0.42	−
3077	100	_[a]	3.5	6.65 ± 0.48	−
3083	112	_[a]	2.3	7.95 ± 0.70	−
3085	208	_[a]	3.7	7.28 ± 0.38	−
3091	210	2.46	4.5	8.80 ± 0.14	−
3094	205	0.01	5.1	6.62 ± 0.39	−
3100	216	_[a]	4.4	9.90 ± 0.11	−

[a] Below limit of detection (0.01 adducts/10^8 nucleotides)

[b] ETS = Environmental Tobacco Smoke exposure, self-reported. “+” = yes, “−” = no

[c] Mean ± SD (n = 3 assays)